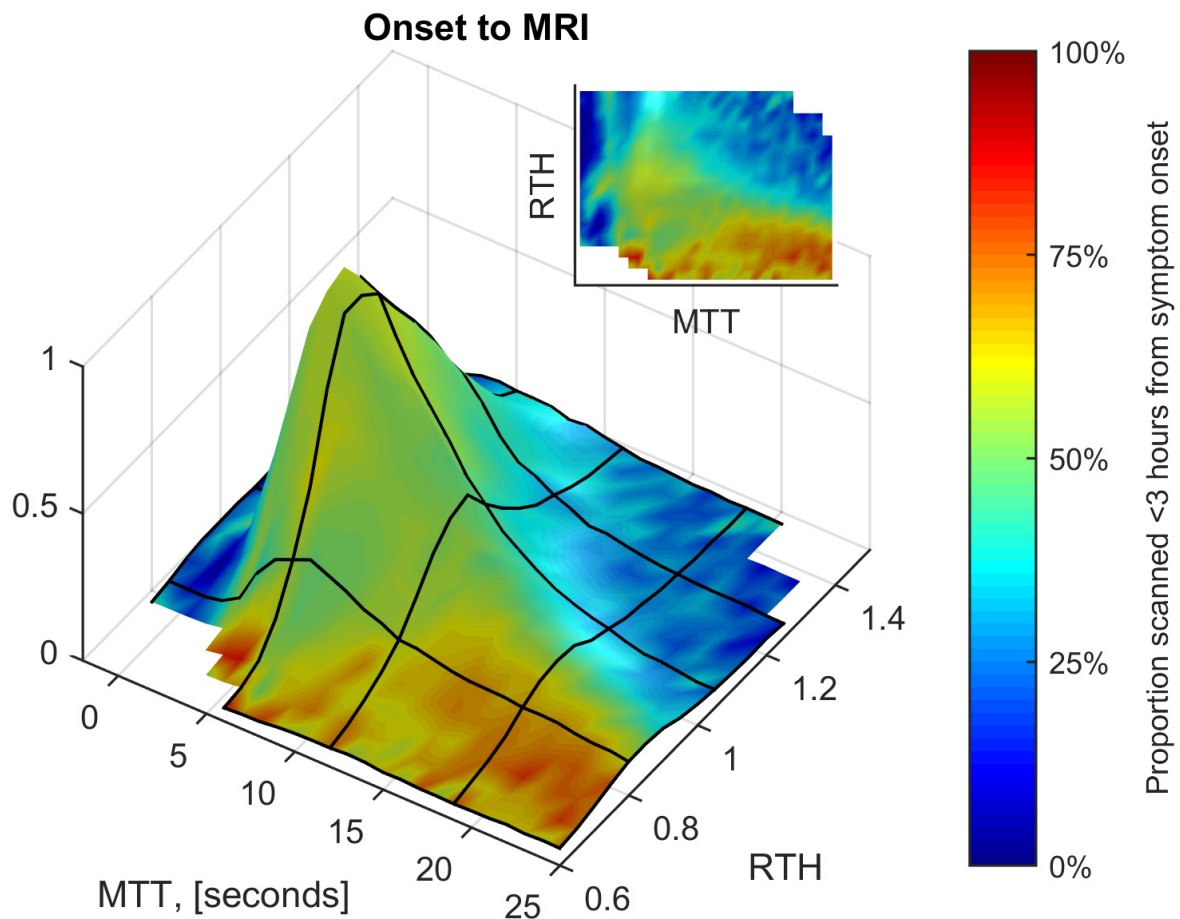
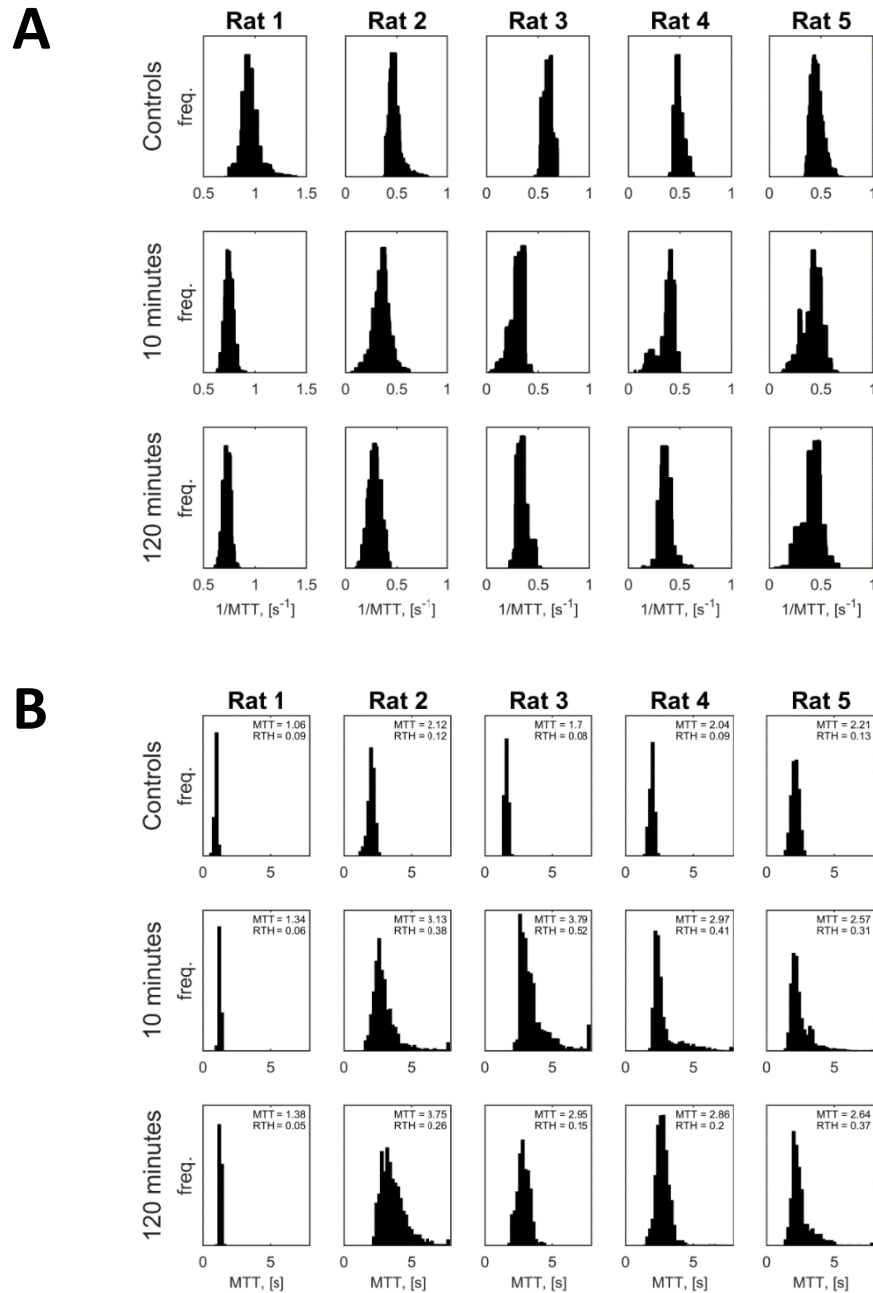


## Supplementary figure 1. Time from onset analysis.



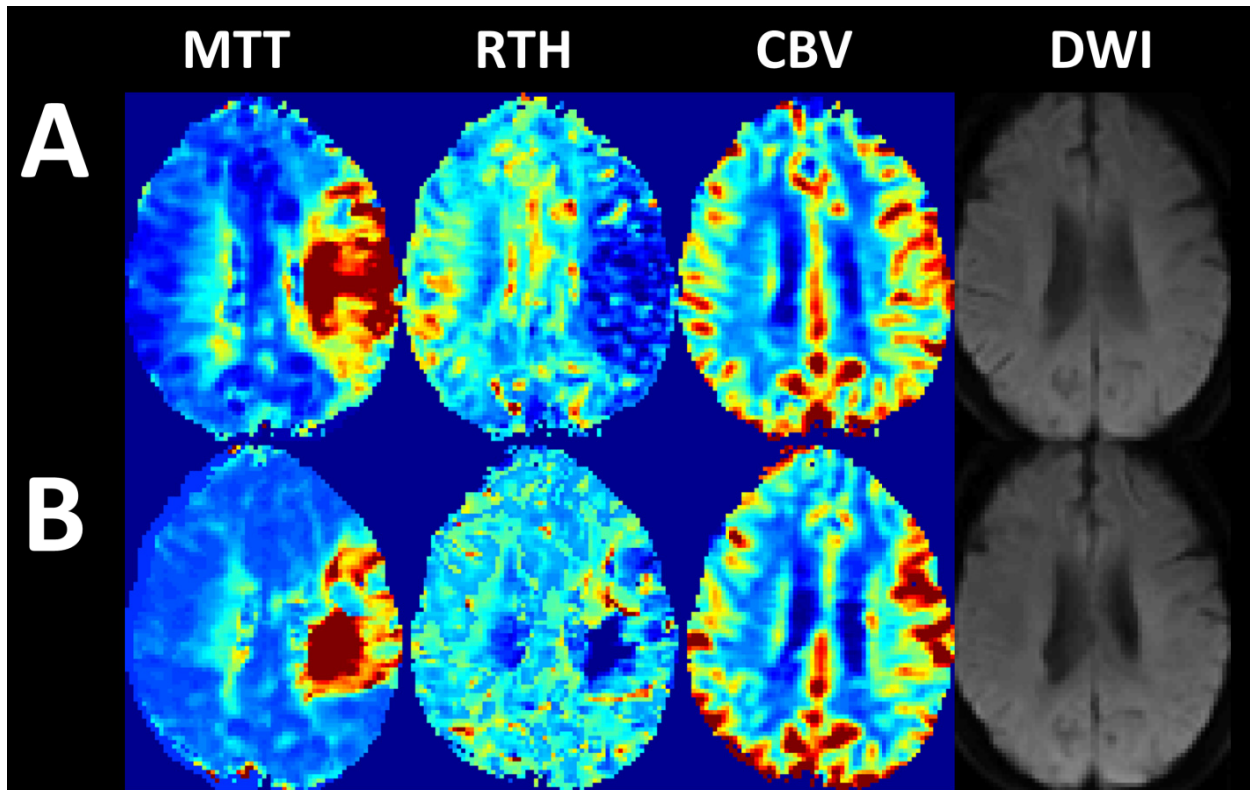
Surface plot illustrating the proportion of tissue that originated from patients scanned within 3 hours of symptom onset (as the surface color) as a function of MTT and RTH. The height of the surface plot indicates the relative proportion of tissue with a given combination of these parameters. All patients with a certain onset time were included ( $N = 90$ ) and the sample was balanced to yield an equal total number of observations for each group (over and under 3 hours, respectively). For a given MTT, voxels with low RTH were more likely to be present before than after 3 hours. While the benefits of recanalizing tissue with long MTT and low RTH are great (Figure 3), this plot underscores the importance of early recanalization.

Supplementary figure 2. Adaptation of figure 4 of Tomita *et al.*<sup>1</sup>



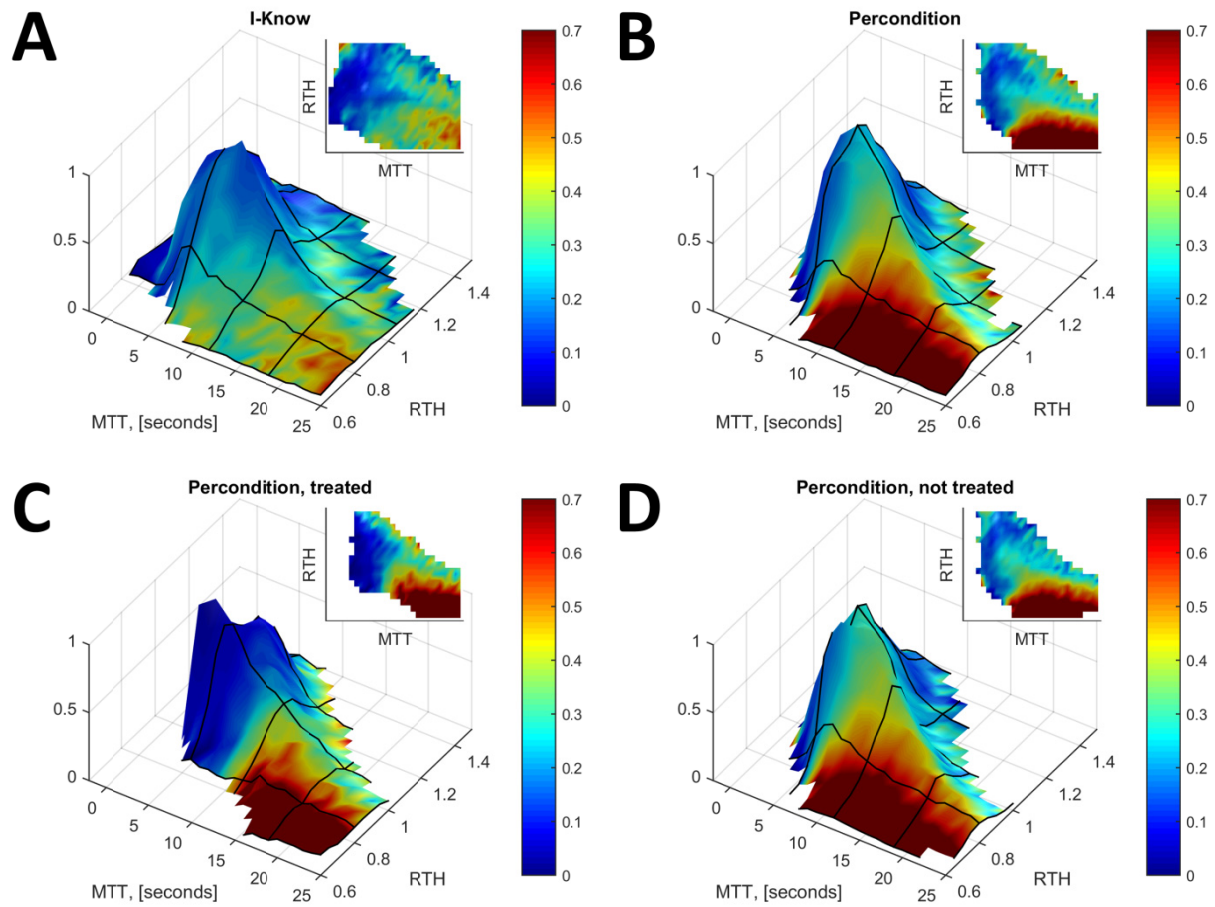
Adapted from Tomita *et al.*<sup>1</sup> (A) Computerized transcription of figure 4 in the paper. (B) Data transformed to present histograms of voxel-wise transit times in the 5 rats. In each histogram the corresponding MTT and RTH value is given. Note the loss of slow flowing capillaries at 120 minutes particularly in rats 3 and 4, corresponding with a dramatic drop in RTH. Mean RTH at the three time-points were (Control: 0.1. 10 minutes of ischemia: 0.33. 120 minutes of ischemia: 0.21).

**Supplementary figure 3. Case.**



Perfusion maps from a patient who presented with an occlusion of his left middle cerebral artery. The acute perfusion lesion volume was 158 mL. The duration between onset and acute MRI (A) was of 1 hour and 23 minutes. Three hours following the acute scan (B), a second MRI was performed. At this time point, the acute occlusion had recanalized (TIMI = 2). No lesion was visible on the DWI map. Only partial reversal of the MTT and RTH lesions are visible, while CBV values are increased. At follow-up, only 7 mL of the acute perfusion lesion had infarcted.

## Supplementary figure 4. Substudies.



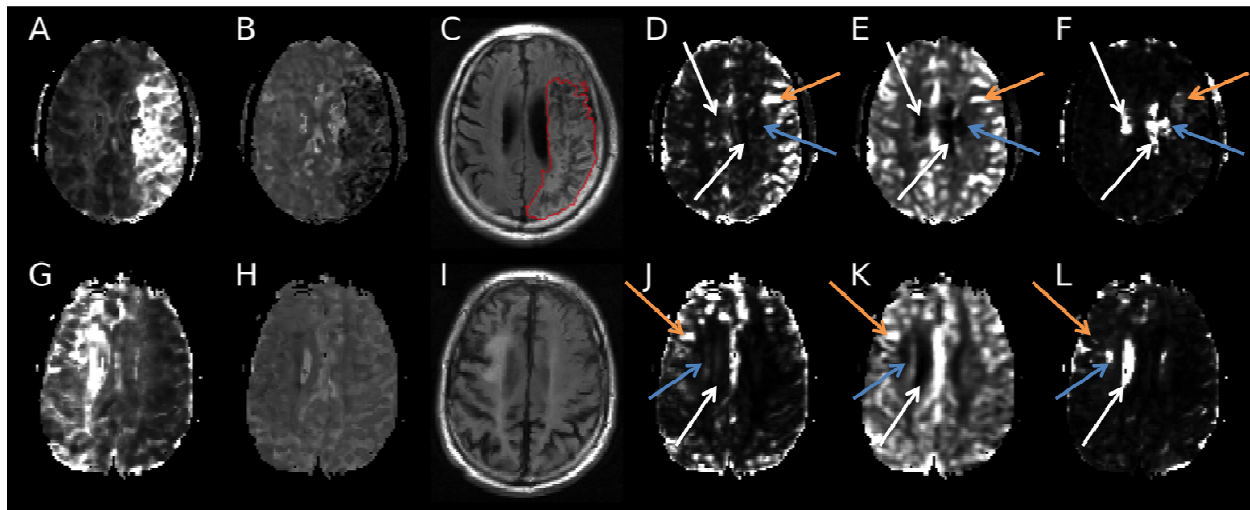
Plots of infarction ratios (as surface colors) as a function of MTT, CTH, and RTH. The heights of the surface plots indicate the relative proportion of tissue with a given combination of these parameters. Plots are limited to patients who did not recanalize at 24 hours. A-B) Depending on study database; I-KNOW and Percondition, respectively. C-D) Percondition database; depending on whether patients were treated with remote perconditioning.

### Supplementary Table 1. Logistic regressions.

Coefficients	$\beta_0$ Intercept	$\beta_1$ R	$\beta_2$ CBF	$\beta_3$ CBV	$\beta_4$ RTH	$\beta_5$ R x CBF	$\beta_6$ R x CBV	$\beta_7$ R x RTH
I-KNOW (N = 79)	-1.3	-1.2	-0.08**	-0.28	-0.50	-1.1	0.26	0.38
Percondition (N = 47)	-0,66	-1.5	-0.20	-0.03*	-0.76	0.29	-0.44	0.38
Percondition status:								
- Treated (N = 23)	-0.60	-1.1	-0.62	0.67	-1.0	0.83	-1.23	0.61
- Un-treated (N = 24)	-0.68	-2.1	-0.02*	-0.29	-0.61	-0.58	0.12	0.30

Logistic regression corresponding to the formula in the results section of the main paper. R is recanalizationstatus at 24 hours (R=1 recanalization; R=0 no recanalization). All p-Values, except those marked with an asterisk, were significant to the value,  $p = 0$ . \*  $p > 0.05$ . \*\*  $p = 0.0001$ . N is the total number of patients in each group.

### Supplementary figure 5. Sum-of-squares of the residuals errors.



Further illustrations of the patient cases from Figure 4 in the manuscript. In this figure, panels A and G are MTT images, panels B and H are RTH images, C and I are follow up FLAIR images with follow up mask overlaid (red contour), D and J are absolute sum-of-squares of the residuals errors (SSE) images, E and K are acute CBV images, while F and L are normalized SSE maps. Visual comparison of the SSE maps (panels D and J) to the CBV maps (panels E and K) indicates a correlation between the SSE and CBV (see yellow arrows in panels D, E, J, and K for examples of high CBV and white arrows for low CBV). This is consistent with SSE being correlated with the amplitude of the underlying curve, i.e. the SSE might be large for two reasons; (i) the fit is poor, which might be attributable to the model being insufficient and/or (ii) the underlying curve has a large amplitude. Panels F and L, show maps resulting from element-wise division of the SSE map with the square of the CBV map, which effectively corresponds to voxel-wise SSE normalization. Revisiting the white arrows in panels F and L, corresponding to low CBV, now display these areas as hyper-intense, which indicate that the fitted model does not approximate the data well. This is not surprising, since the arrows point to cerebrospinal fluid (CSF) areas, which have low (zero) CBV and hence low absolute SSE, while the normalized SSE is large. Similarly, the large CBV, large absolute SSE areas (yellow arrows) are effectively removed on the normalized SSE map. The blue arrows identify regions with low absolute SSE, which are, however, hyperintense on the normalized SSE maps. These regions likely represent diffusion lesions, and correspond well with these masks of the original figure. Since the region of interest of the current study was the perfusion/diffusion mismatch, this bias is limited in our sample. In the region between the blue arrow and yellow arrow in patient A, there might be an unexplained residual SSE, indicative of the gamma approximation being insufficient in fitting the data. However, this area is comparatively, very small.

1. Tomita Y, Tomita M, Schiszler I, et al. Moment analysis of microflow histogram in focal ischemic lesion to evaluate microvascular derangement after small pial arterial occlusion in rats. *J Cereb Blood Flow Metab* 2002; 22: 663-669.